Available online at www.sciencedirect.com
SCIENCE DIRECT®
Geochimica et Cosmochimica Acta 70 (2006) 548–561
Geochimica
www.elsevier.com/locate/gca

Temperature and its control of isotope fractionation by a sulfate-reducing bacterium

Donald E. Canfield [a,*], Claus A. Olesen [a,b], Raymond P. Cox [b]

[a] Nordic Center for Earth Evolution (NordCEE) and Institute of Biology, University of Southern Denmark, Campusvej 55, 5230, Odense M, Denmark
[b] Department of Biochemistry and Molecular Biology, University of Southern Denmark, Campusvej 55, 5230, Odense M, Denmark

Received 25 January 2005; accepted in revised form 12 October 2005

Abstract

A synthesis of previous results, which we dub the "standard model," provides a prediction as to how isotope fractionation during sulfate reduction should respond to physiological variables such as specific rate of sulfate reduction and environmental variables such as substrate availability and temperature. The standard model suggests that isotope fractionation should decrease with increasing specific rates of sulfate reduction (rate per cell). Furthermore, the standard model predicts that low fractionations should be found at both high and low temperatures whereas the highest fractionations should be found in the intermediate temperature range. These fractionation trends are controlled, as a function of temperature, by the balance between the transfer rates of sulfate into and out of the cell and the exchange between the sulfur pools internal to the organism. We test this standard model by conducting experiments on the growth physiology and isotope fractionation, as a function of temperature, by the sulfate-reducing bacterium *Desulfovibrio desulfuricans* (DSMZ 642). Our results contrast with the "standard model" by showing a positive correlation between specific rates of sulfate reduction and fractionation. Also by contrast with the standard model, we found the highest fractionations at low and high temperatures and the lowest fractionations in the intermediate temperature range. We develop a fractionation model which can be used to explain both our results as well as the results of the "standard model." Differences in fractionation with temperature relate to differences in the specific temperature response of internal enzyme kinetics as well as the exchange rates of sulfate in and out of the cell. It is expected that the kinetics of these processes will show strain-specific differences.

1. Introduction

Sulfate-reducing prokaryotes are well known to fractionate sulfur during sulfate reduction (Thode et al., 1951; Harrison and Thode, 1958; Kaplan and Rittenberg, 1964; Chambers et al., 1975; Habicht and Canfield, 1997). Taken together, the extent of measured fractionations ($\varepsilon_{\text{sulfate–sulfide}}$) ranges between about 0 and 46‰ (see summary in Canfield, 2001a). Part of this variability is due to inherent differences among species (Detmers et al., 2001), and some is also due to environmental variables such as electron donor supply, sulfate availability and temperature (Harrison and Thode, 1958; Kaplan and Rittenberg, 1964; Habicht et al., 2002). Among individual species of sulfate reducers, reduced fractionations have been noted at high specific rates of sulfate reduction (rate per cell) (Harrison and Thode, 1958; Kaplan and Rittenberg, 1964; Kemp and Thode, 1968; Chambers et al., 1975). As specific rates of sulfate reduction increase with increasing temperature (within an organism's growth range), increasing temperature is frequently also linked with reduced fractionations (Harrison and Thode, 1958; Ohmoto and Felder, 1987; Canfield, 2001b). Fractionations are also reduced at low sulfate concentrations of less than about 200 μM (Harrison and Thode, 1958; Habicht et al., 2002).

With both high specific rates of sulfate reduction and low sulfate concentrations, reduced fractionations are explained by the influence of sulfate limitation on isotope

* Corresponding author.
E-mail address: dec@biology.sdu.dk (D.E. Canfield).

0016-7037/$ - see front matter © 2005 Elsevier Inc. All rights reserved.
doi:10.1016/j.gca.2005.10.028

fractionation. Thus, as the argument goes, at high temperatures when rates of sulfate reduction are high, and at low sulfate concentrations, the transport of sulfate across the cell membrane becomes the rate-limiting step. There is little isotope fractionation associated with this step (Kaplan and Rittenberg, 1964), and if it becomes rate limiting, then the greater fractionations associated with the intracellular reduction steps will not be expressed (e.g Harrison and Thode, 1958; Kaplan and Rittenberg, 1964; Rees, 1973). Lower fractionations have also been noted at temperatures approaching the minimum for growth for individual sulfate-reducing strains (Kaplan and Rittenberg, 1964; Kemp and Thode, 1968; Canfield, 2001b). At low temperatures, membrane fluidity is reduced (Scherer and Neuhaus, 2002), which may also limit sulfate transport across the membrane resulting in reduced fractionations. These generalizations on the controls of isotope fractionation by sulfate reducers can be viewed as the "standard model." Our purpose here is to test this standard model. We do so here by exploring the fractionations during sulfate reduction by a *Desulfovibrio* strain across its whole temperature range for growth. By doing so, we can assess the relative influence of sulfate exchange across the cell membrane, and internal cellular processes, on isotope fractionation through the growth temperature range. Surprisingly, the "standard model" does not explain our results.

2. Further background and fractionation model

2.1. Biochemistry of sulfate reduction process

Our results will be interpreted in light of the internal biochemical and physical pathways associated with the sulfate reduction process. These are outlined above, but considered in more detail here.

During dissimilatory sulfate reduction (meaning sulfate reduction associated with energy metabolism) marine strains of sulfate reducers using sulfate concentrations at greater than around 100 μM bring sulfate into the cell together with 2 Na^+ ions (see review in Cypionka, 1995). This is accomplished by special membrane-bound symport proteins, and the process is reversible. The activity of membrane-bound proteins is expected to be temperature sensitive (Scherer and Neuhaus, 2002). At low temperatures, membrane fluidity is reduced (Hochachka and Somero, 1984), and cells compensate by increasing the low molecular weight complement of membrane fatty acids and by increasing the relative amounts of unsaturated fatty acids (e.g. Scherer and Neuhaus, 2002). These adaptations with temperature have been observed by Rabus et al. (2002) for the psychrotolerant *Desulfobacterium autotrophicum* grown between 4 and 28 °C. At low enough temperatures, however, the membrane will become too rigid for membrane-bound proteins to function. At high temperatures, membrane fluidity increases and membrane-bound proteins become less encumbered. Still, cells must combat the potential destabilizing effects of high temperature, and they do this by increasing their complement of high molecular weight fatty acids and by increasing the proportions of saturated fatty acid (Scherer and Neuhaus, 2002). At high enough temperature, the membrane becomes too unstable and the cell will lyse.

Once inside the cell, sulfate is reduced to sulfide through a number of enzyme-mediated steps. The first is the activation of sulfate to adenosine phosphosulfate (APS) through the enzyme ATP sulfurylase (Eq. (1)):

$$SO_4^{2-} + ATP + 2H^+ \leftrightarrow APS + PP_i \quad (1)$$

With a $\Delta G^{o'}$ of 46 kJ mol^{-1} (value at pH 7, but otherwise standard state) this reaction is quite endergonic, and PPi is rapidly hydrolyzed making the whole process favorable (Cypionka, 1995). This step is reversible, as is the next step, the reduction of APS to sulfite. This reaction is catalyzed by the enzyme APS reductase, and it is shown in Eq. (2) with H_2 as the electron donor:

$$APS + H_2 \leftrightarrow HSO_3^- + AMP + H^+ \quad (2)$$

This reaction is exergonic with a $\Delta G^{o'}$ of −69 kJ mol^{-1}.

From here, sulfite is generally assumed to proceed straight to sulfide with the enzyme dissimilatory sulfite reductase (Eq. (3)):

$$SO_3^{2-} + 3H_2 + 2H^+ \rightarrow H_2S + 3H_2O \quad (3)$$

This reaction is also exergonic with a $\Delta G^{o'}$ of −174 kJ mol^{-1} (Cypionka, 1995), and it is believed that most of the energy is conserved during sulfate reduction through this step. There is, however, some evidence that the reduction of sulfite to sulfide may proceed, at least under some circumstances, through a variety of steps; the so called trithionate pathway (e.g. Akagi, 1995). Here, sulfite is first reduced to trithionate by sulfite reductase (Eq. (4)). Trithionate is then reduced to thiosulfate with the enzyme trithionate reductase (Eq. (5)), and finally, thiosulfate is reduced to sulfide through thiosulfate reductase (Eq. (6)). All of these steps are exergonic with $\Delta G^{o'}$ values, in order, of −48, −122, and −4 kJ mol^{-1}.

$$3SO_3^{2-} + H_2 + 4H^+ \rightarrow S_3O_6^{2-} + 3H_2O \quad (4)$$

$$S_3O_6^{2-} + H_2 \rightarrow S_2O_3^{2-} + SO_3^{2-} + 2H^+ \quad (5)$$

$$S_2O_3^{2-} + H_2 \rightarrow H_2S + SO_3^{2-} \quad (6)$$

Whether dissimilatory sulfite reduction proceeds predominantly in one step (Eq. (3)), or in multiple steps (Eqs. (4)–(6)), is currently unknown (see Rabus et al., 2000).

Also unknown is the extent to which the step(s) between sulfite and sulfide are reversible. Sulfite reductase enzymes are involved in oxidative metabolisms, and they are responsible for the oxidation of sulfide to sulfite in phototrophic and chemotrophic sulfide-oxidizing organisms (e.g., Dahl and Trüper, 1994). However, efforts to document such reversibility between sulfite and sulfide during sulfate reduction have thus far proven futile (Kemp and Thode, 1968). Brunner and Bernasconi (2005) have recently developed an isotope fractionation model incorporating

the trithionite pathway, which also allows the steps in this pathway to be reversible. This model is conceptually rigorous and generates a more complex reaction network than we explore below. However, the importance of the trithionite pathway remains uncertain as does is the reversibility of the steps in the pathway. Due to the complexity of their network and the uncertainty of the pathways in it, we have no means of rigorously evaluating our results with the Brunner and Bernasconi (2005) model. In our modeling, then, we adopt a simpler approach and assume that sulfite reduction proceeds directly from sulfite to sulfide in a single step and that this step is not readily reversible. If sulfite reduction proceeds through multiple pathways (Eqs. (4)–(6)), and if the reactions are reversible with associated fractionations, then the formalities of our analysis will need to be changed. However, our main conclusions will remain robust concerning the relative significance of internal enzyme processes versus membrane exchange in controlling fractionation.

2.2. Sulfur isotope model

As described briefly in Section 1, the fractionations expressed during sulfate reduction will depend greatly on which steps limit the sulfate reduction process. Thus, if sulfate exchange across the cell membrane is the rate-limiting step, then most, if not all, of the sulfate entering the cell will be reduced and minimal fractionation will be expressed. On the other hand, the largest fractionations will be expressed if the last step in the process is rate limiting, and if the various intermediates along the path are rapidly reversible. In this case, all of the fractionations associated with the individual steps will be expressed (Rees, 1973).

Based on the principles outlined above, we construct a model which can be used to interpret our isotope results. The model is similar in spirit to the one developed by Rees (1973), but uses Hayes (2001) and Farquhar et al. (2003) as its formal starting points. Farquhar et al. (2003) describes a reaction network for sulfate reduction as follows:

$$SO_{4(out)} \underset{2,\varphi 2}{\overset{1,\varphi 1,\alpha 1}{\rightleftharpoons}} \left[SO_{4(in)} \underset{5a}{\overset{4a}{\rightleftharpoons}} APS \underset{5b,\varphi 5}{\overset{4b,\varphi 4,\alpha 4}{\rightleftharpoons}} SO_3 \right] \xrightarrow{3,\varphi 3,\alpha 3} H_2S \qquad (7)$$

The numbers designate the various steps, φ represents mass flow, and α is the fractionation factor associated with the steps where fractionations apply. Within this network, branching points can be defined describing both the exchange of sulfate across the cell membrane, as well as the exchange of reaction intermediates in the internal cycling of sulfur. The first branching point differentiates the internal and external cell environment. With this branch point, the mass flow of sulfur into the cell matches the mass flow out of the cell:

$$\varphi_1 = \varphi_2 + \varphi_3. \qquad (8)$$

The fraction of sulfur exiting the cell as sulfide compared to the total amount of sulfur entering the cell is given by:

$$f_3 = \frac{\varphi_3}{\varphi_2 + \varphi_3}. \qquad (9)$$

When f_3 approaches 1, there is little flow of sulfate back through the cell membrane out of the cell, and when f_3 is low, most of the sulfate entering the cell exits it again. A second branch point describes the extent to which the step forming sulfite is reversible. In this case, the mass flow of sulfur to sulfite is equal to the mass flow of sulfur back towards sulfate plus the mass flow of sulfur to sulfide.

$$\varphi_4 = \varphi_5 + \varphi_3. \qquad (10)$$

Only a fraction of the sulfite formed from sulfate is further reduced to sulfide, and this fraction is given by f_5[1]:

$$f_5 = \frac{\varphi_3}{\varphi_5 + \varphi_3}. \qquad (11)$$

Thus, if f_5 is large, most of the sulfite formed from sulfate is further reduced to sulfide, and as f_5 approaches 0, there is more exchange between sulfate and sulfite. Note that f_5 refers to the overall transfer between sulfate and sulfite, but not necessarily the values for the individual steps in pathways 4 or 5. For example, if exchange between sulfate and APS was very rapid, then, the exchange between sulfate and sulfite would be controlled by steps 4b and 5b. On the other hand, if the exchange between APS and sulfite was very rapid, but there was little exchange between sulfate and APS, then the overall exchange between sulfate and sulfite would be controlled by steps 4a and 5a. As no fractionation is believed to accompany the formation of APS from sulfate (Rees, 1973), these two species should have the same isotopic composition. If fractionation did occur during between sulfate and APS, then an additional branching point would need to be specified.

From the equalities presented above, and isotope mass balance (see Appendix A), expressions can be written describing the influence of f_3 and f_5 on the isotopic composition of sulfide resulting from sulfate reduction. The first expression describes the internal isotopic composition of sulfate in the cell:

$$rSO_{4(in)} = \frac{rH_2S + rH_2S - f_5 rH_2S + \alpha_3 f_5 rH_2S}{\alpha_4[\alpha_3 + \alpha_3 rH_2S + f_5 rH_2S - \alpha_3 f_5 rH_2S]}. \qquad (12)$$

In this expression r represents the isotope ratio ($^{34}S/^{32}S$) for the species of interest. Isotope ratio can be converted to isotopic compositions relative to an isotope standard, which is normally Cañon Diablo troilite, with the expression

$$\delta^{34}S = \left[\frac{r_{sample}}{r_{std}} - 1\right] \times 1000. \qquad (13)$$

[1] Our definition of f_5, is somewhat different, but related, to the definition used by Farquhar et al. (2003). From Farquhar $f_5 = \varphi_5/(\varphi_3 + \varphi_5)$, and thus describes the fraction of sulfite which is **NOT** further reduced to sulfide. When our $f_5 = 1$, the f_5 from Farquhar is 0, and vice versa. For our purpose, the definition used here is more logical as both f_3 and f_5 are defined for forward processes, and in particular both are defined relative to the same parameter which is the flow of sulfide out of the cell, φ_3.

In our calculations we use 0.0441638 as the $^{34}S/^{32}S$ ratio of the standard, which is the value for the Vienna Cañon Diablo troilite standard (Ding et al., 2001). The following expression relates the isotopic composition of sulfate outside the cell to the isotopic composition of sulfate in the cell:

$$rSO_{4(out)} = \frac{rSO_{4(in)} + rSO_{4(in)}rH_2S - f_3rSO_{4(in)} + f_3rH_2S}{\alpha_1[1 + rH_2S + f_3rSO_{4(in)} - f_3rH_2S]}. \quad (14)$$

To analyze the relationship between f_3, f_5, and $\delta^{34}S_{H_2S}(r_{H_2S})$ we first fix values for f_3 and f_5. We then choose rH_2S, which gives us values for $rSO_{4(in)}$ (Eq. (12)), and these are inserted in Eq. (13) to recover the given value for $rSO_{4(out)}$. Thus, rH_2S values are chosen by trial and error until the correct $rSO_{4(out)}$ is recovered.

3. Methods

3.1. Culture conditions

All experiments were performed with the brackish-water strain *Desulfovibrio desulfuricans* (DSMZ 642). The cells were vibrio shaped with an average length of 4 μm and an average width of 0.7 μm. Cultures were grown on sterilized modified DSMZ medium 194, which, in one liter of water, contained: 5 g $NaHCO_3$, 3 g Na_2SO_4 (21 mM), 20 g NaCl, 0.4 g $MgCl_2 \cdot 6H_2O$, 0.5 g KCl, 0.2 g KH_2PO_4, 0.3 g NH_4Cl, 0.15 g, 0.15 g $CaCl_2 \cdot 2H_2O$, 0.75 g resazurin, 1 g yeast extract, and as organic substrate, 2.78 ml of 50% Na-lactate (15.9 mM). Also included was 1 ml of sterilized trace metal solution (SL-10), containing in one liter: 10 ml 7.7 M HCl, 1.5 g $FeCl_2 \cdot 4H_2O$, 70 mg $ZnCl_2$, 100 mg $MnCl_2 \cdot 4H_2O$, 6 mg H_3BO_3, 190 mg $CoCl_2 \cdot 6H_2O$, 2 mg $CuCl_2 \cdot 2H_2O$, 24 mg $NiCl_2 \cdot 6H_2O$ and 36 mg $Na_2MoO_4 \cdot 2H_2O$. To this was added 10 ml of sterilized vitamin solution containing in one liter: 2 mg biotin, 2 mg folic acid, 5 mg pyridoxine–HCl, 5 mg thiamine–$HCl \cdot 2H_2O$, 5 mg riboflavin, 5 mg nicotinic acid, 5 mg D-Ca-pantothenate, 0.1 mg vitamin B_{12}, and 5 mg *p*-aminobenzoic acid and 5 mg lipoic acid. This medium was reduced with 0.5 mM Na_2S.

The culture was grown in batch mode at 28 °C, and transferred regularly until the start of the temperature block experiments. A series of 70, 16 mm (OD) by 125 mm tall gas-tight culture tubes, containing 9 ml of anoxic sterile medium (and a headspace of 10% CO_2 and 90% N_2), were rapidly inoculated with 1 ml of culture in the late exponential growth phase. Two of these tubes were immediately harvested as controls (see below for details of tube harvesting). The tubes used for incubation were quickly transferred to an aluminum temperature gradient block (Isaksen and Jørgensen, 1996) maintained at −1 °C in the cold end and 40 °C in the warm end. The tubes were placed, in quadruplicate, at approximately 2 °C intervals in pre-drilled holes along the block, which was enclosed in 5-cm thick insulating foam. Temperature was monitored continuously at the cold end of the block, at the center, and at the hot end, and it remained stable (±1 °C at the cold end, decreasing to ±0.1 °C at the hot end) throughout the whole 150 day duration of the experiment.

Growth was measured regularly by turbidity (see below) and tubes were harvested at different phases of growth. The first tubes were taken during the middle of the exponential growth phase (tube a) and this ranged from a few hours to several weeks after start of the incubation, depending on the temperature as it controlled growth rate. Tubes were also taken late in the exponential growth phase (tube b), early in the stationary phase (tube c), and late in the stationary growth phase (tube d). A preliminary experiment was run to help decide the timing of sample collection, which was especially important for the fastest-growing cultures. On removal from the block, 1.1 ml of culture was extracted through the rubber septum on the top of the tube and transferred to a 1.5 ml Eppendorf centrifuge tube. The samples from the Eppendorf tube were quickly filtered through 0.2 μm Nalgene OEM PVDF filters or centrifuged at 3500 rpm at 4 °C. In both cases, the liquid phase was collected and frozen for later analysis of sulfate concentration, as well as for dissolved organic acid content (lactate, acetate, formate). The remainder of the culture was fixed with one milliliter 20% (w/w) $ZnCl_2$. These samples were frozen for later sulfide concentration and isotope analyses. The $ZnCl_2$ arrested cellular metabolism (Fossing and Jørgensen, 1989) and fixed the sulfide as insoluble ZnS. Furthermore, freezing stabilizes the ZnS which slowly oxidizers in air. Freezing does not negatively affect sulfide concentration measurements; in fact, in our experience, ZnS particles become more finely distributed after a freeze–thaw cycle and are easier to sub-sample without bias. In some cases, 900 μl of culture was collected and fixed in 100 ml 25% gluteraldehyde for later DAPI (4′-6-diamidino-2-phenylindole) staining and cell counting.

The optical density of all culture tubes was monitored frequently using a system constructed of an Ultrabright 1000mCD light-emitting diode light source (λ_{max} 660 nm) opposite a photodiode at the same level (Cox et al., 1989). The signal intensity of the photodiode was calibrated with cultures of known cell density and further, with $BaSO_4$ suspensions of known concentration (McFarland standard). The reproducibility of the photodiode measurements depended on cell density. With cell densities of $>\approx 10^8$ cells ml^{-1}, the reproducibility of replicate measurements was about 3%. At 5×10^7 cells ml^{-1} reproducibility dropped to about 15%, and below 2×10^7 cells ml^{-1} noise in the photodiode rendered optical density measurements unreliable.

3.2. Chemical analyses

Sulfide was collected from the $ZnCl_2$-fixed culture tubes by distilling about half the content of the tubes (the rest was stored and used if needed) in 6 N HCl, and trapping

the evolved H_2S as Ag_2S in $AgNO_3$ solution. The Ag_2S was collected on filters, rinsed with distilled water and dried. The acid solution in the distillation apparatus was filtered through a GFF glass fiber filter, and the sulfate in the filtrate was precipitated as $BaSO_4$ after adding one milliliter 1 M $BaCl_2$ and heating to boil to aid crystal development (Canfield, 1989). The Ag_2S and $BaSO_4$ samples, including the culture controls processed in the same way, were analyzed for S isotopic composition by first combustion to SO_2 gas with an elemental analyzer, and then passing the purified SO_2 gas through an isotope-ratio mass spectrometer. Isotopic compositions are reported relative to the Cañon Diablo-Vienna Troilite standard with a standard deviation of ±0.3‰.

Sulfide concentrations were determined on small subsamples of the $ZnCl_2$-fixed cultures with the colorimetric methylene-blue method (Cline, 1969). Standard deviation is estimated at 10%. Sulfate concentrations (±2%) were determined on ultra-centrifuged samples collected from the culture tubes immediately after harvesting (see above) by ion chromatography on a Sykam ion chromatograph with column suppression. Concentrations of lactate, acetate, and formate (±5%) were measured by ion chromatography using a Sykam chromatograph with column HPX-87H (Bio-Rad) and UV detection at 210 nm. Before running, the samples were diluted tenfold in a 5 mM H_2SO_4 buffer.

4. Results

From our organic acid analyses, sulfate reduction proceeded with the expected stoichiometry (Eq. (15)), and no formate was formed, as can occur with some incomplete oxidizing sulfate-reducing prokaryotes (Habicht et al., 2005).

$$2C_3H_6O_3 + SO_4^{2-} + 2H^+ \rightarrow 2C_2H_4O_2 + H_2S + 2CO_2 + 2H_2O \quad (15)$$

By comparing cell numbers measured with DAPI to the corresponding optical densities measured with our photodiode, we generated a calibration curve from which all of our optical density measurements could be converted to cell densities. From these results a series of growth curves were generated, with a typical example, from the tubes incubated at 17.9 °C, shown in Fig. 1. The cell harvesting times are also shown, and in this case, as was general for the experiment, the growth trends in the replicate tubes were very similar. Specific growth rates, μ (h^{-1}) (±3% for all temperatures except 7 °C, where the uncertainty was ±15%), were calculated during the exponential growth phase from:

$$\mu = \frac{\ln N - \ln N_0}{t}, \quad (16)$$

where N_0 is the cell density at the start of the exponential growth phase, and N is the cell density at time t in hours. As expected, cell growth responded strongly to temperature and increased until about 32 °C, where a general plateau was observed (Fig. 2A). Below 7 °C, some growth occurred in the cultures, but it was slow, and an exponential growth phase could not be identified. In most cases, growth stopped when lactate was exhausted, and sulfate reduction could no longer occur.

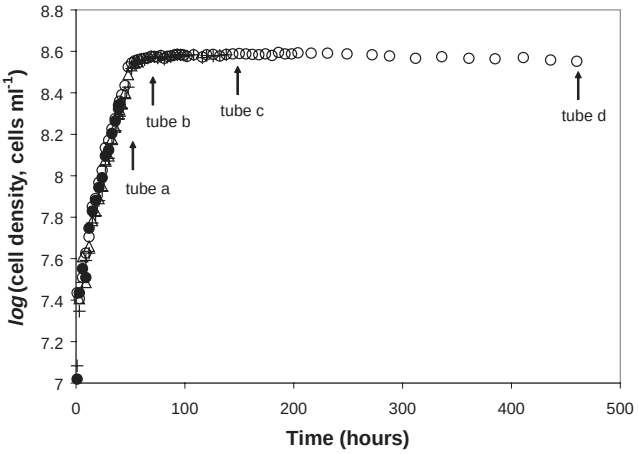

Fig. 1. The natural log of cell density with time for the experiment at 17.9 °C. Also shown is the cell harvesting times for the 4 tubes incubated at this temperature.

Rates of sulfate reduction (±4%) were calculated during the exponential phase of growth (up to the time where the "b" sample was harvested) as the change in sulfate concentration divided by the time elapsed when the tube was harvested. The trend with temperature was very similar to the specific growth rate (Fig. 2B). Specific rates of sulfate reduction (rate per cell, ±6%) were calculated during the exponential growth phase by dividing the sulfate reduction rate with the cell numbers observed at the end of the exponential growth phase. These rates also correlate with temperature in a similar manner to specific growth rates and volume-based rates of sulfate reduction (Fig. 2C).

Growth yield expresses the amount of cell material produced per amount of substrate used, and it provides an indication of the metabolic efficiency of the organism. This could be of interest in interpreting fractionation patterns. High growth yields mean that the energy or carbon derived from growth substrates is efficiently channeled into biomass production, whereas low growth yields mean less efficient substrate utilization. Growth yields do not generally parallel specific growth rates or cell-specific rates of substrate utilization (e.g. Isaksen and Jørgensen, 1996). From our experiments, growth yield (millions of cells/μmol lactate used) was calculated by dividing the cell numbers (millions of cells cm^{-3}) generated at the point of complete lactate consumption by the concentration of lactate used (μmol cm^{-3}). This calculation provided similar, though more certain (±3%), results than for growth yield calculated just during the exponential growth phase (±8%). For growth yields calculated during the exponential growth period uncertainties in the lactate concentration measurements add to the uncertainties of the growth yield calculation. At the lowest temperatures, lactate was not completely

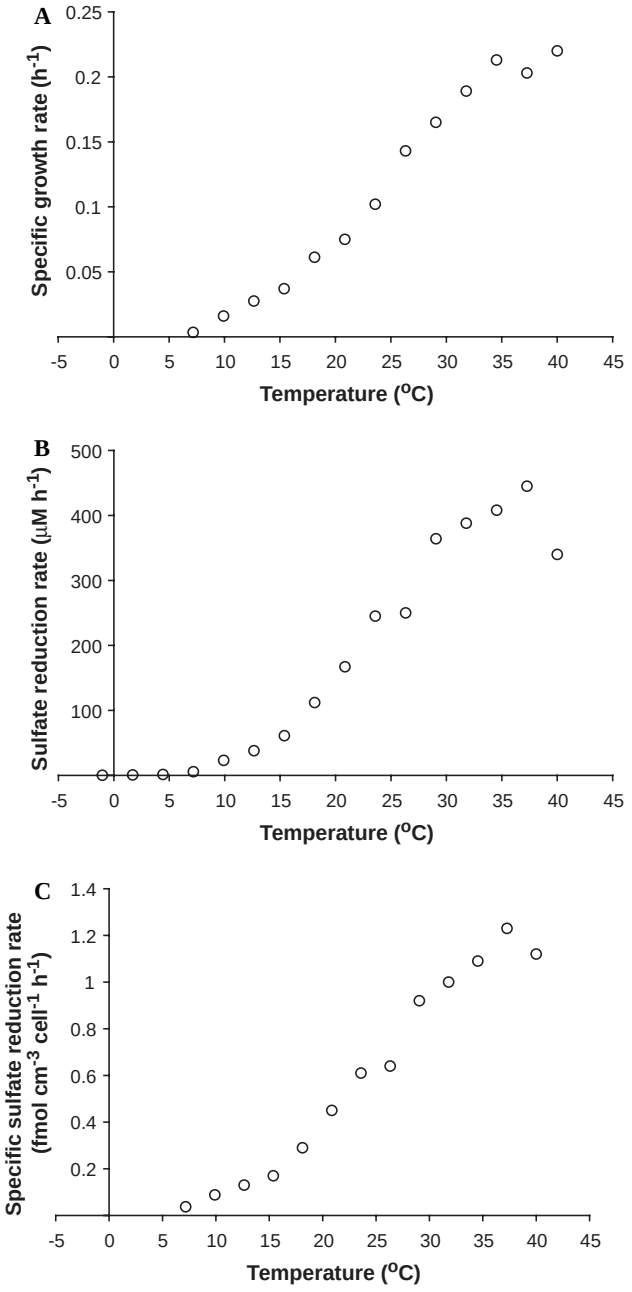

Fig. 2. (A) Specific growth rate of the sulfate-reducing culture as a function of temperature (uncertainty of ±3% for all temperatures except 7 °C, where the uncertainty was ±15%), (B) rates of sulfate reduction (rate per volume, ±4%) as a function of temperature, and (C) specific rates of sulfate reduction (rate per cell, ±6%) as a function of temperature. Rates were calculated from tube b measurements taken at the end of the exponential growth phase.

used, and growth yield (±8%) was calculated by dividing the cell numbers at the end of the experiment with the total amount of lactate used. The results are shown in Fig. 3. Growth yields were low at low temperature, and they increased to a broad plateau between 17 and 32 °C. At higher temperatures they again began to decrease. The deviations at high and low temperatures are defined by relatively few points, but they are also well outside of analytical uncertainty.

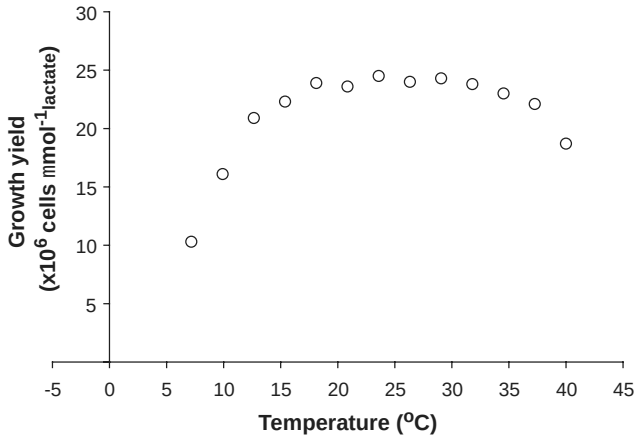

Fig. 3. Growth yield (millions of cells per μmol of lactate oxidized, ±3%, increasing to ±8% at the lowest two temperatures shown) as a function of temperature. Experiments were performed down to −1 °C, but the growth was too slow, and the uncertainties in cell numbers too great, to allow reliable growth yield calculations.

Isotope fractionation during sulfate reduction (±0.5‰) was determined with a Rayleigh distillation model from the measured isotopic compositions of sulfide and sulfate, and the relative concentration changes in sulfide and sulfate during the incubation. Fractionations were independently calculated from both the sulfate and the sulfide data. For fractionations calculated from sulfate, the following formulation was used (e.g. Canfield, 2001a):

$$\alpha_{SO_4\text{–}H_2S} = 1 + \frac{[\ln(\delta_{SO_4\text{-start}} + 1000) - \ln(\delta_{SO_4\text{-end}} + 1000)]}{\ln(f_{SO_4})}, \quad (17)$$

where $\alpha_{SO_4\text{–}H_2S}$ is the fractionation factor between sulfate and sulfide, $\delta_{SO_4\text{-start}}$ is the isotopic composition of sulfate at the beginning of the experiment, $\delta_{SO_4\text{-end}}$ is the isotopic composition of sulfate at the time of sampling, and f_{SO_4} is the fraction of the original sulfate remaining.

During the course of the incubation, the isotopic composition of sulfide develops in relationship to the isotopic composition of sulfate:

$$\delta_{SO_4\text{-end}} = \frac{(\delta_{SO_4\text{-start}} - \delta_{H_2S\text{–}SR} f_{H_2S})}{f_{SO_4}}, \quad (18)$$

where, in addition to the terms already defined, $\delta_{H_2S\text{–}SR}$ is the isotopic composition of sulfide added by sulfate reduction, and f_{H_2S} is the fraction of the original starting sulfate converted into sulfide ($f_{H_2S} + f_{SO_4} = 1$). To calculate fractionations from the sulfide data, $\delta_{H_2S\text{–}SR}$ was substituted into Eq. (18), from which $\delta_{SO_4\text{-end}}$ was calculated. This, in turn, was substituted into Eq. (17), from which fractionations were calculated. Values for $\delta_{H_2S\text{–}SR}$ were corrected for the small amount of sulfide transferred with the original inoculum and used to reduce the medium and therefore:

$$\delta_{H_2S\text{–}SR} = \frac{\delta_{H_2S\text{-total}}[H_2S_{total}] - \delta_{H_2S\text{-start}}[H_2S_{start}]}{[H_2S_{SR}]}, \quad (19)$$

where $\delta_{H_2S\text{-total}}$ is the isotopic composition of sulfide measured at the time of sampling and $[H_2S_{total}]$ is its concentration. Likewise, $\delta_{H_2S\text{-start}}$ is the isotopic composition of sulfide at the start of the incubation including inoculum and the sulfide used to reduce the medium, $[H_2S_{start}]$ is its concentration, and $[H_2S_{SR}]$ is the concentration of sulfide added from sulfate reduction ($[H_2S_{total}] = [H_2S_{start}] + [H_2S_{SR}]$).

The fractionations calculated from these equalities are presented in Fig. 4. There is a small systematic difference in the fractionations calculated from the sulfide and sulfate results, where the fractionations from sulfide are on average about 0.3‰ depleted in ^{34}S compared to those from sulfate. We do not understand in detail the cause of his systematic difference. The Rayleigh distillation model should be robust for this type of experiment as should the correction for the isotopic composition and concentration of sulfide at the start of the experiment. There could be possible systematic biases in the sulfide and sulfate isotopic measurements. We have not, however explored for this. In any event, the differences are small and have no influence on our interpretations of the fractionation results.

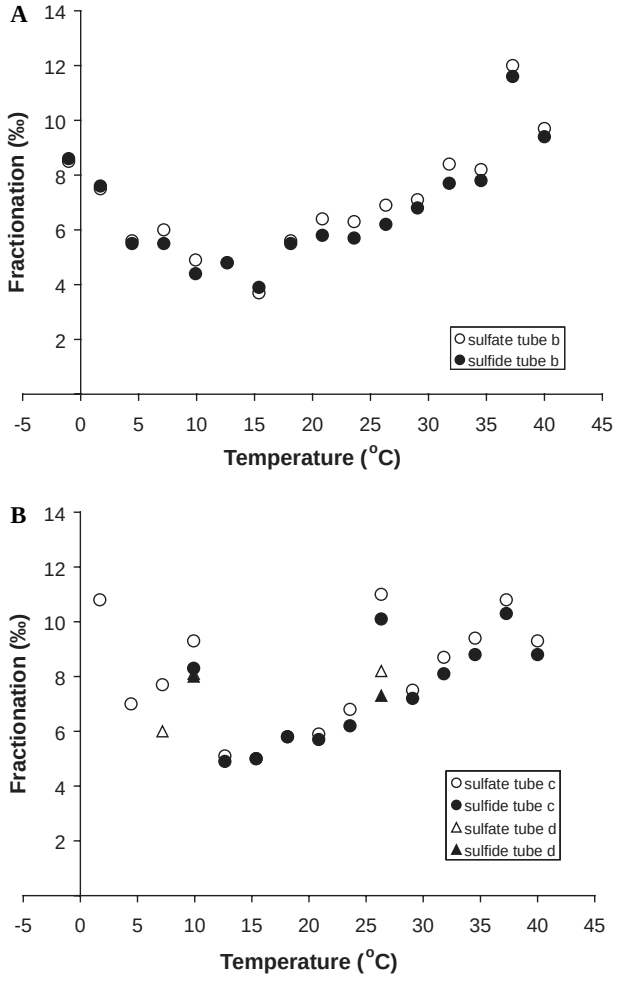

Fig. 4. Isotope fractionation during sulfate reduction (±0.5‰) as a function of temperature. (A) for tubes collected in the late exponential growth phase, with fractionations calculated both from sulfate and sulfide data, and (B) for tubes collected in the stationary growth phase with, as in (A), fractionations calculated from both sulfate and sulfide data.

For tubes collected during the late exponential growth phase (Fig. 4A) a regular trend of relatively high fractionations is observed at the lowest temperatures, decreasing to about 15 °C. After this, fractionations increased again with increasing temperature, with an apparent decrease at the highest temperature explored. Fractionations recorded in the stationary growth phase (tubes c and d) (Fig. 4B) generally followed the same pattern, although in a couple of instances, unexpectedly high fractionations were encountered. At the lower temperatures for tube c, the sulfide samples were unfortunately lost so no isotope analyses could be performed.

5. Discussion

5.1. Growth physiology

As outlined in Section 1, the standard model suggests that isotope fractionation during sulfate reduction should be influenced in predictable ways by the physiology of the sulfate reducer as controlled by factors such as substrate availability and temperature. Temperature is the control factor explored here. Thus, we will begin by discussing how temperature influenced the growth physiology of *D. desulfuricans* strain DSMZ 642, after which we will consider further how growth physiology might have influenced our fractionation results.

The *Desulfovibrio* strain used in this study is a typical *Desulfovibrio* species. Its size is typical with an average diameter of 0.7 μm and a length of 3–4 μm. Furthermore, like all *Desulfovibrio* species, it oxidizes lactate incompletely producing equimolar amounts of acetate and CO_2 (see Eq. (15)). Strain DSMZ 642 has a temperature optimum for growth in the range of 35–40 °C (Fig. 2), which is in the higher end for other known *D. desulfuricans* strains (e.g. Widdel, 1988). Strain DSMZ 642 has a high maximum specific growth rate, μ, of 0.22 h^{-1}, giving a doubling time of 3.3 h during exponential growth. Such high growth rates have also been reported for strains of *Desulfovibrio vulgaris* growing on H_2 (Widdel, 1988). The growth rate of strain DSMZ 642 responded to temperature according to the Arrhenius equation within the temperature range of 10–32 °C (Fig. 5A), which is expressed in natural log form as:

$$\ln \mu = \ln A - \frac{E_a}{RT}, \tag{20}$$

where A is a constant, E_a is an "apparent" activation energy (kJ mol^{-1}), R is the gas constant (8.31 K^{-1} mol^{-1}), and T is temperature. Microorganisms, including sulfate reducers, exhibit an Arrhenius temperature response to growth when growing within their optimal growth range (e.g. Ingraham and Marr, 1996; Isaksen and Jørgensen, 1996;

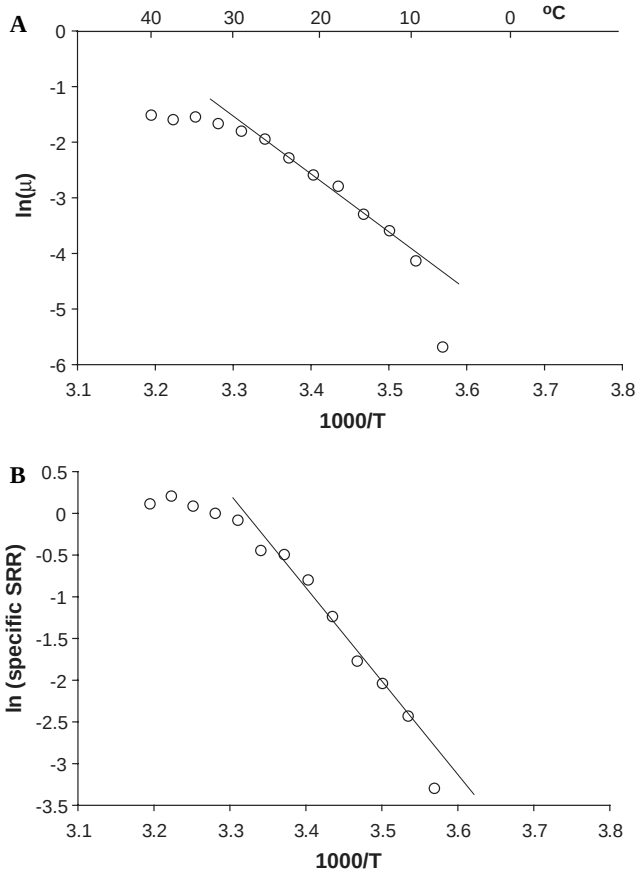

Fig. 5. Trends in: (A) the natural log of specific growth rate (μ, h^{-1}), and (B) the natural log of specific rates of sulfate reduction (fmol cm^{-3} $cell^{-1}$ h^{-1}), as a function of $1/T$, with T in K. The lines represent the temperature range where specific rates of growth and specific rates of sulfate reduction responded to the Arrhenius equation. See text for details.

Knoblauch and Jørgensen, 1999). From the trend in Fig. 5A, an "apparent" activation energy of 89.0 kJ mol^{-1} is calculated, which is not unusual for sulfate reducers (Isaksen and Jørgensen, 1996; Knoblauch and Jørgensen, 1999).

There is a large drop in growth rate between 10 and 7 °C, suggesting that below 10 °C, growth was especially inhibited. This trend is only well supported by one point, but the drop is steep, and it is consistent with the general behavior of microorganisms growing at the low end of their temperature range (Ingraham and Marr, 1996). It seems possible that at low temperatures the rigidity of the cell membrane limits transport into and out of the cell and therefore limits growth rate. From the growth yield results (Fig. 3), a reduction of metabolic efficiency was observed at 10 °C becoming particularly acute at 7 °C. Thus, from both specific growth rates and growth yield, metabolic performance was restricted below 10 °C. Deviations from an Arrhenius dependence on growth were also observed at temperatures above 32 °C (Fig. 5A). At approximately this same temperature growth yield also began to drop (Fig. 3), but not severely. The drop in metabolic efficiency above 32 °C could be related to the increased channeling of energy into cellular repair as temperature increases and cellular components become unstable. It could also be related to the specific temperature response of critical enzymes in the cellular metabolism of the organism.

The cell-specific rates of sulfate reduction measured here (Fig. 2C) spanned a range quite typical for *D. desulfuricans* strains in particular (e.g. Kaplan and Rittenberg, 1964) and sulfate reducers in general (see Canfield et al., 2000 for a summary). Our *Desulfovibrio* strain also responded to temperature in a similar manner to growth following the Arrhenius equation in the range of 10–32 °C with an "apparent" activation energy, E_a, of 85.6 kJ mol^{-1}. Also like specific growth rate, they deviated from this trend at higher and lower temperatures (Fig. 5C). Similar to growth, then, the drop in specific rates of sulfate reduction below 10 °C likely resulted, at least in part, from stiffening of the cell membrane and the restriction of membrane-bound transporter enzymes. At high temperatures (above 30 °C), rates of sulfate reduction could have been hindered by increasing cellular damage, or by the specific kinetic temperature response of key enzymes in the sulfate reduction process, as also discussed above for specific growth rate. Since the energy for growth comes from sulfate reduction, it is no surprise that specific rates of growth and specific rates of sulfate reduction correlated closely together.

5.2. Isotope fractionation

The isotope fractionation produced during sulfate reduction by *D. desulfuricans* strain DSMZ 642 ranged in total from 4‰ to 12‰. This range in fractionations is lower than those observed for other *D. desulfuricans* strains where fractionations up to 46‰ have been observed (Kaplan and Rittenberg, 1964), and fractionations in the range of 20‰ are common (Kaplan and Rittenberg, 1964; Kemp and Thode, 1968; Chambers et al., 1975). However, our fractionations are generally higher than those measured by Detmers et al. (2001) for a variety of different *Desulfovibrio* species, although *D. desulfuricans* was not included in their survey. Some of these differences in the magnitude of fractionation, when comparing among studies, could be due to differences in growth conditions. For example, in the study of Detmers et al. (2001), cells were grown under optimal conditions, whereas Kaplan and Rittenberg (1964) measured fractionations on resting cell suspensions, and Chambers et al. (1975) measured fractionations in continuous culture. However, there may also be real strain-specific differences in the fractionation among, ostensibly, the same species. This latter hypothesis could be tested by examining a variety of different strains of the same "species" under identical conditions.

As our study focused specifically on the influence of temperature on fractionation, it is most instructive to review our temperature trends in fractionation with the predictions of the standard model. In the standard model, low temperatures and stiffening of the cell membrane reduce

sulfate transport across the membrane and thereby produce a reduction in fractionation. The results of Kaplan and Rittenberg (1964) are consistent with this model, where they found low fractionations for their *D. desulfuricans* strain growing at low temperatures of 5–10 °C, when compared to fractionations at higher temperatures. Also, Canfield (2001b) found that fractionations at 5 °C were lower when compared to 25 °C for natural populations of sulfate reducers growing on both acetate and ethanol. No temperature effect on fractionation, however, was observed when the populations were grown on lactate. Finally, Brüchert et al. (2001) observed lower fractionations at 4 °C compared to 20 °C for the psychrophilic sulfate-reducing strain ASv20 growing on acetate. However, other psychrophilic strains showed no or little temperature effect on fractionation (Brüchert et al., 2001). Thus, the results of the present experiment differ from the predictions of the standard model, and from a body of evidence (but not all evidence) from pure cultures and natural populations of sulfate reducers.

What about at high temperatures? In the standard model, high temperatures produce reduced fractionations. This is because accelerating rates of sulfate reduction increase sulfate demand by the cell, preferentially channeling sulfate to sulfide, reducing exchange out of the cell. Again, some observations support this model. Kaplan and Rittenberg (1964) as well as Harrison and Thode (1958) found generally reduced fractionations at high temperatures where sulfate reduction rates were high. Indeed, from these studies, and others (Kemp and Thode, 1968; Chambers et al., 1975), one observes an inverse correlation between cell-specific rates of sulfate reduction and fractionation (see summary in Canfield, 2001b). This would also be consistent with the standard model, but contrasts with the trends between specific rates of sulfate reduction and fractionation observed here (Fig. 6). Finally, Canfield (2001b) observed a strong decrease in fractionation for natural populations of sulfate reducers when temperature was increased from 25 to 35 °C. A large increase in sulfate reduction rate accompanied this temperature change, and the overall response was, therefore, consistent with the standard model. By contrast, in our experiments, isotope fractionation continuously increased with increasing temperature and specific rates of sulfate reduction. This response, as at low temperatures, is also at odds with the standard model.

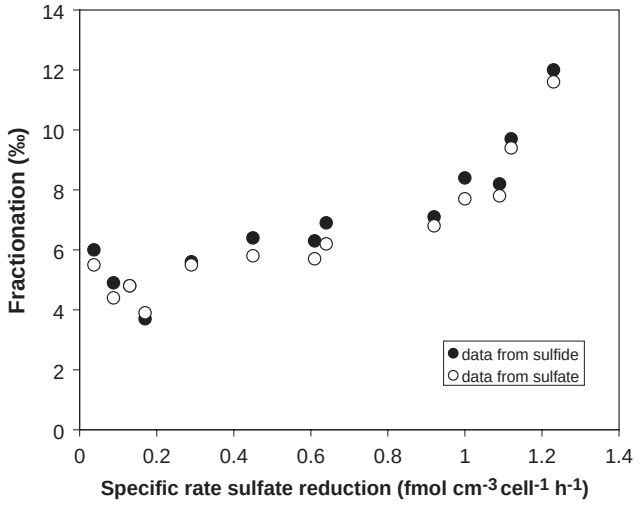

Fig. 6. Specific rates of sulfate reduction plotted against isotope fractionation for tubes harvested in the late exponential growth phase. Fractionations have been calculated both from sulfate and sulfide data.

Overall, our results display fractionation trends with metabolic activity (specific growth rate and specific rates of sulfate reduction) and temperature that are different from those observed previously and from those predicted from the standard model. Part of these differences could relate to strain-specific differences in the controls on fractionation with temperature. More studies of the type conducted here could help identify between-strain differences in controls on fractionation. Our results, clearly show that fractionation trends can display internally consistent patterns that are not predictable based on our previous understanding of the main factors controlling fractionation. Our challenge, therefore, is to explain both our observations, and those of the standard model. The quantitative fractionation model developed above is the backdrop for this comparison.

5.3. Quantitative fractionation model

We will explore our fractionation trends with temperature using the general model developed above for isotope fractionation by sulfate reducers. However, we start by exploring some of the model features and predictions. As described above, and elsewhere (e.g. Harrison and Thode, 1958; Kaplan and Rittenberg, 1964; Rees, 1973; Farquhar et al., 2003), the specifics of mass flow through reaction networks exert a profound control on the expression of isotope fractionation. Specifically, both the network associated with transfer of sulfate in and out of the cell, f_3, and the network associated with the exchange of the internal sulfate pool with sulfite, f_5, can significantly control fractionation.

In using our model we assume, as did Rees (1973), a fractionation ($\varepsilon_{\mathrm{sulfate_{out}-sulfate_{in}}}$) of −3‰ for the transport of sulfate into the cell (α_1 in Eq. (7)), and 25‰ for each of the steps of APS to sulfite (α_4 in Eq. (7)) ($\varepsilon_{\mathrm{sulfate_{in}-APS}}$), and sulfite to sulfide (α_3 in Eq. (7)) ($\varepsilon_{\mathrm{sulfite-sulfide}}$). Brunner and Bernasconi (2005) have suggested much larger fractionations for the step from sulfite to sulfide. This arises from their interpretation of the fractionation results of Detmers et al. (2001), where, in particular, relatively high fractionations of 36.7‰ were observed for the rapidly metabolizing *Desulfobacula phenolica*. In the view of Brunner and Bernasconi (2005) such rapid metabolism would by necessity yield (in our parlance) high values for f_3 and f_5. This, in their view, would require higher than normally described values for the internal fractionation steps to maintain the reasonably high observed fractionation. This is possible,

but in our opinion not yet proven. Indeed, there may be a range of species-specific fractionations associated with the different enzymatic steps in the sulfate reduction process. This would be an interesting area of future research. In what follows we will use the values originally proposed by Rees (1973), recognizing that other values may be more appropriate and that there may be variability between different sulfate-reducing organisms. The specific choice of the individual fractionations will not, however, significantly influence our interpretations of the present fractionation results nor the conclusions offered below.

From Eqs. (12) and (14) we can calculate how the overall fractionation ($\varepsilon_{\text{sulfate}_{\text{out}}-\text{sulfide}}$) will respond to changes in f_3 and f_5 and these results are shown in Fig. 7. Starting with Fig. 7A, when f_5 is low, allowing maximum exchange between the internal sulfate pool and sulfite, fractionation is very sensitive to f_3, the transfer of sulfate in and out of the cell. Under these circumstances, the maximum possible fractionation (the sum of all the individual fractionations, equal to 47‰ relative to the external sulfate pool) is observed when f_3 is also low. The isotopic composition of sulfide is always offset by 50‰ compared the internal sulfate pool, and the isotopic composition of this pool varies linearly with f_3. When f_3 is constant and low (Fig. 7B), maximum fractionations, as before, are also expressed when f_5 is low. However, even when f_5 is 1, a fractionation of 22‰ (relative to the external sulfate pool) is still expressed.

Importantly, even with the same overall fractionation, the isotopic composition of the internal sulfate pool can vary depending on specific values of f_3 and f_5. A careful evaluation of the isotopic composition of the internal sulfate pool can, in fact, fix the values of f_3 and f_5. The isotopic composition of this sulfate pool has never been determined, but we can obtain unique solutions for f_3 and f_5 from Eqs. (12) and (14):

$$f_3 = \frac{\alpha_1 r\mathrm{SO}_{4(\mathrm{out})} - \alpha_1 r\mathrm{SO}_{4(\mathrm{out})} r\mathrm{H_2S} + r\mathrm{SO}_{4(\mathrm{in})} + r\mathrm{SO}_{4(\mathrm{in})} r\mathrm{H_2S}}{\alpha_1 r\mathrm{SO}_{4(\mathrm{out})} r\mathrm{SO}_{4(\mathrm{in})} - \alpha_1 r\mathrm{SO}_{4(\mathrm{out})} r\mathrm{H_2S} + r\mathrm{SO}_{4(\mathrm{in})} - r\mathrm{H_2S}}, \tag{21}$$

$$f_5 = \frac{\alpha_3\alpha_5 r\mathrm{SO}_{4(\mathrm{in})} + \alpha_3\alpha_5 r\mathrm{SO}_{4(\mathrm{in})} r\mathrm{H_2S} - r\mathrm{H_2S} - r^2\mathrm{H_2S}}{r\mathrm{H_2S}(\alpha_3\alpha_5 r\mathrm{SO}_{4(\mathrm{in})} - \alpha_5 r\mathrm{SO}_{4(\mathrm{in})} + \alpha_3 - 1)}. \tag{22}$$

With a knowledge of $r_{\mathrm{SO}_{4(\mathrm{in})}}$ (the isotopic composition of the internal sulfate pool) and all of the internal fractionations (α values), Eqs. (21) and (22) are completely constrained giving unique values of f_3 and f_5.

With this general background we can try to explore fractionation trends with temperature by mixing the influences of f_3 and f_5 as we might expect them to respond to temperature. We will begin with trying to explain the standard model. The standard model suggests that transfer across the cell membrane controls fractionation at low temperatures (f_3), while the conversion efficiency of the internal sulfate pool to sulfide (f_5) limits fractionation at high temperatures. From the standard model, then, f_3 should be high at low temperature and decrease with increasing temperature, while f_5 should be low at low temperatures and increase with increasing temperature. An example of how f_3 and f_5 might vary with temperature, consistent with

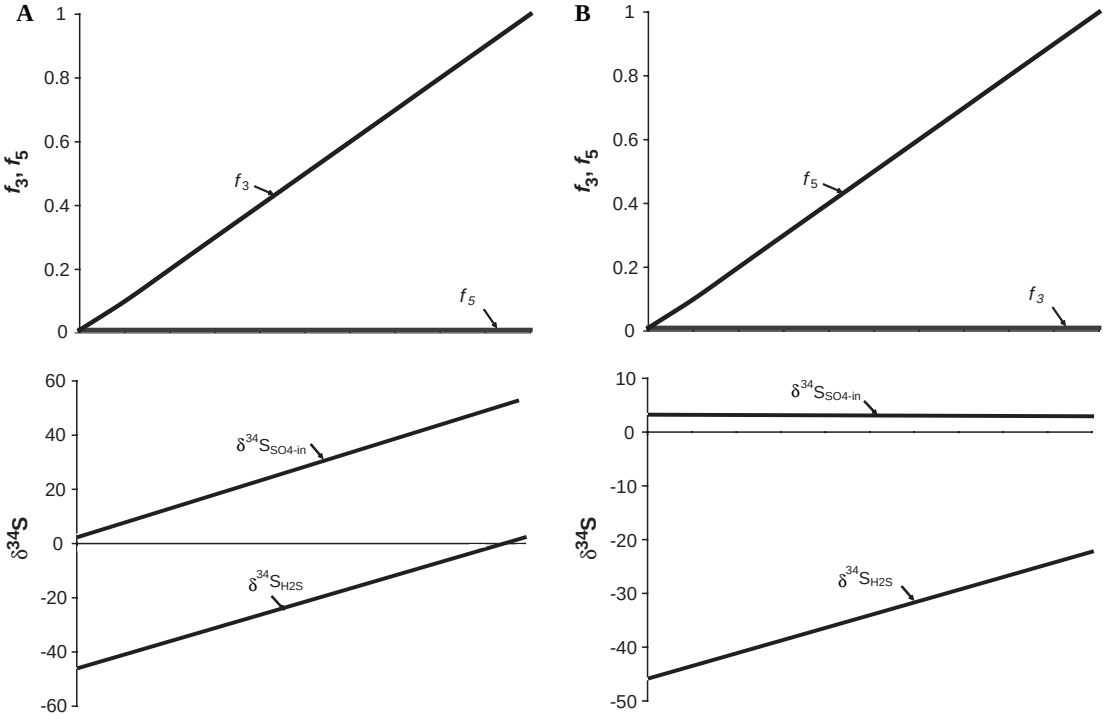

Fig. 7. Model trends in the isotopic composition of the internal sulfate pool ($\delta^{34}S_{SO_{4(in)}}$), and sulfide produced during sulfate reduction ($\delta^{34}S_{H_2S}$) with different relationships between f_3 and f_5. See text for details.

the standard model, is shown in Fig. 8A. In this figure, proceeding from left to right represents an increase in temperature. Using the same internal cellular fractionations as in Fig. 7, the trends in fractionation with "temperature" are consistent with the standard model: smallest at low and high temperatures, and highest in between.

However, alternative trends in f_3 and f_5 could also satisfy the general prediction that f_3 should decrease and f_5 should increase with increasing temperature. These basic conditions are also satisfied in Fig. 8B, and in this case the fractionation trend resembles the one from our results (compare to Fig. 4). Thus, trends in fractionation with temperature, and controls of fractionation in general, depend to a large measure on the exact relationships between f_3 and f_5. With this view, the standard model and those results supporting it, represent a particular style of relationship between f_3 and f_5, but not the only one consistent with the general condition that f_3 should decrease and f_5 should increase with increasing temperature.

The results in Fig. 8 are rather general and are not meant to reproduce the fractionations we observed in our experiments. However, through further exploration of the model, we were able to reproduce our experimental trends while still preserving the internal fractionations used in Figs. 7 and 8 (Table 1). Thus, in principle, low fractionations, and the trends we observed between fractionation and temperature, are reproduced through judicious choice of f_3 and f_5. We can view these choices as yet untested predictions as to the magnitude of f_3 and f_5 with different temperatures in our experiment.

Table 1
Values of f_3 and f_5 to satisfy experimental results

Temperature	f_3	f_5	Fractionation
Low	0.75	0.05	9.5
Medium	0.75	0.8	4.8
High	0.55	0.8	12.3

The relatively high values of f_3 required to match the model predictions with isotope results (Table 1) suggest that there was at all temperatures a rather limited exchange between the internal and external sulfate pools. By contrast, the low values of f_5 at low temperature suggest that the internal sulfate pool is in near exchange equilibrium with sulfite. This would occur if the reduction of sulfite to sulfide was particularly sluggish. As temperature increases into the intermediate and high range, increasing values of f_5 suggest that the reduction rate of sulfite to sulfide increases dramatically relative to the exchange rate between the internal sulfate and sulfite pools. At the same time, a commensurate fall in f_3 requires that the transfer rates of sulfate in and out of the cell increases more strongly with increasing temperature than the reduction rate of sulfite to sulfide. Our physiological data seems to support this as increasing temperature above about 32 °C

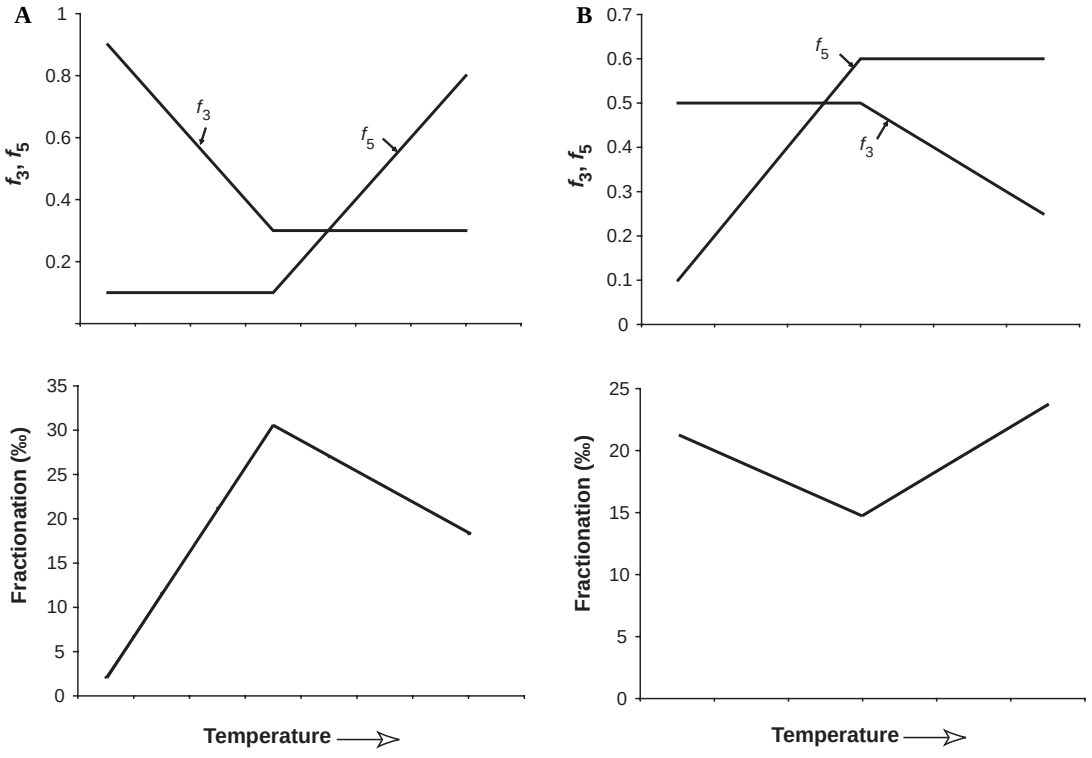

Fig. 8. Model trends in isotope fractionation during sulfate reduction with different relationships between f_3 and f_5. The x-axis, moving from left to right, is meant to represent increasing temperature. The trends in (A) represent those expected from the standard model, whereas the trends in (B) represent the results from the present study. Even though f_3 and f_5 break slope at the same point in this analysis, there is no assumption that this is necessarily true. These trends are purely hypothetical and meant to reproduce the overall predictions of the standard model as well as the present results. See text for details.

had little effect on specific rates of sulfate reduction, yet, presumably, increasing temperature increased membrane fluidity and the transfer rates of substances across the cell membrane.

Overall, our fractionation results suggest that different parts of the sulfate reduction apparatus responded differently to temperature. Thus, in our experiments, the exchange rates of sulfate across the cell membrane and the reduction rate of sulfite to sulfide apparently responded more strongly to temperature than the exchange rate between the internal sulfate and sulfite pools. These responses are not universal because for sulfate reducers following the standard model, the opposite must be true. More broadly, our results show how different combinations of f_3 and f_5 have a decided influence on isotope fractionation during sulfate reduction. In addition, our results and associated model provide a template by which we can further understand the fractionation process. In particular, we point to the internal sulfate pool as an important constraint on the relative importance of f_3 and f_5 in controlling fractionation. This work is not yet been accomplished, but should be a high priority.

6. Conclusions

We have explored isotope fractionation accompanying sulfate reduction by the sulfate reducer *D. desulfuricans* strain DSMZ 642 as a function of temperature through the whole temperature range where the organism metabolizes and grows. Different temperatures encourage different metabolic rates and different degrees of metabolic efficiency. Previous work on sulfate-reducing populations suggests that membrane stiffening at the low end of the organism's temperature range will reduce sulfate transfer rates across the membrane ultimately limiting the degree of fractionation. Higher fractionations might be expected in the intermediate temperature range, and lower fractionations are expected again at the high temperature end where rapid rates of cellular metabolism are believed to limit the exchange between the internals sulfur pools. Our goal was to test the predictions of this "standard model" and to come further in understanding the processes controlling isotope fractionation by sulfate reducers.

In our experiments, *D. desulfuricans* strain DSMZ 642 fractionated between about 4 and 12‰ during sulfate reduction. This range in fractionations is lower than found in earlier work on isotope fractionation during sulfate reduction by *Desulfovibrio* strains, but our growth conditions were also different. Importantly, we found high fractionations at low temperatures, the lowest fractionations in the intermediate temperature range and high fractionations again at the highest temperatures. These results are not consistent with the standard model. We constructed a quantitative fractionation model considering mass flows of sulfur through various branch points in the sulfate reduction pathway and the associated fractionations. We found that we could easily reproduce the trends in the standard model, as well as our own, depending in the exact relationship between the extent to which: (1) sulfate is transferred into and out of the cell, and (2) the extent to which sulfur exchanges between the internal sulfur pools. Thus, different sulfate-reducing populations balance the magnitudes of these two exchange paths in different ways as a function of temperature. It is difficult, therefore, to predict a priori how temperature will affect fractionation, but our results also open the door to a better general understanding of the processes controlling the extent of fractionation by sulfate-reducing organisms.

Acknowledgments

We thank Peter Søholt and Lilian Salling for expert assistance in the laboratory, and we thank Poul Esbensen and Bent Bach Andersen for help with the construction of the gradient temperature block. Our work was improved by the insightful comments of three anonymous GCA reviewers and by Tim Lyons. Finally, we thank the Danish National Science Foundation (Danmarks Grundforskningsfond) for their generous support.

Associate editor: Timothy W. Lyons

Appendix A

We begin, as does Farquhar et al. (2003), by considering a hypothetical, simple, reaction network with a single branching point as expressed in Eq. (A.1):

$$\mathrm{A} \underset{2,\varphi 2,\alpha 2}{\overset{1,\varphi 1,\alpha 1}{\rightleftharpoons}} \mathrm{B} \xrightarrow{3,\varphi 3,\alpha 3} \mathrm{H_2S}. \tag{A.1}$$

As in the main text, φ represents mass flow, and α is the fractionation factor associated with each step. We consider the major isotopes of S, ^{32}S and ^{34}S (Farquhar et al., 2003, also considered the minor S isotopes ^{33}S and ^{36}S), and we follow the transfer of ^{34}S through step 1, which is related to the transfer through steps 2 and 3:

$$^{34}n_1 = {}^{34}n_2 + {}^{34}n_3, \tag{A.2}$$

where n is the number of atoms of isotope ^{34}S transferred. We can recast the number of atoms transferred as an isotope ratio such that, for example:

$$^{34}n_1 = \varphi_1 \frac{^{34}n_1}{^{32}n_1 + {}^{34}n_1}. \tag{A.3}$$

With $r_1 = {}^{34}n_1/{}^{32}n_1$, Eq. (A.3) may be rewritten as:

$$^{34}n_1 = \varphi_1 \frac{r_1}{1 + r_1}. \tag{A.4}$$

With this equality, Eq. (A.2) may be recast as follows:

$$\varphi_1 \frac{r_1}{1 + r_1} = \varphi_2 \frac{r_2}{1 + r_2} + \varphi_3 \frac{r_3}{1 + r_3}. \tag{A.5}$$

From here, we consider the reaction network presented in the text (Eq. (7)), slightly simplified without the APS intermediate (see text for details):

$$SO_{4(out)} \underset{2,\varphi 2,\alpha 2}{\overset{1,\varphi 1,\alpha 1}{\rightleftarrows}} \left[SO_{4(in)} \underset{5,\varphi 5,\alpha 5}{\overset{4,\varphi 4,\alpha 4}{\rightleftarrows}} SO_3 \right] \xrightarrow{3,\varphi 3,\alpha 3} H_2S. \quad (A.6)$$

If we consider the branching point around SO_3^{2-}, and by analogy with Eq. (A.5), the following equality can be written:

$$\varphi_4 \frac{r_4}{1+r_4} = \varphi_5 \frac{r_5}{1+r_5} + \varphi_3 \frac{r_3}{1+r_3}. \quad (A.7)$$

From mass balance $\varphi_4 = \varphi_3 + \varphi_5$, and as in the text, we define:

$$f_5 = \frac{\varphi_3}{\varphi_3 + \varphi_5} = \frac{\varphi_3}{\varphi_4}. \quad (A.8)$$

With the equalities in Eq. (A.8), we eliminate the mass flow terms in Eq. (A.7).

$$\frac{r_4}{1+r_4} = \frac{(1-f_5)r_5}{1+r_5} + \frac{f_5 r_3}{1+r_3}. \quad (A.9)$$

We also note the following equalities:

$$r_1 = rSO_{4(out)}\alpha_1, \quad (A.10)$$

$$r_2 = rSO_{4(in)}, \quad (A.11)$$

$$r_4 = rSO_{4(in)}\alpha_4, \quad (A.12)$$

$$r_5 = rSO_3, \quad (A.13)$$

$$r_3 = rSO_3\alpha_3 = rH_2S, \quad (A.14)$$

$$r_5 = rH_2S/\alpha_3. \quad (A.15)$$

Eqs. (A.12), (A.14), and (A.15) are substituted into (A.9), yielding:

$$\frac{rSO_{4(in)}\alpha_4}{1+rSO_{4(in)}\alpha_4} = \frac{(1-f_5)\frac{rH_2S}{\alpha_3}}{1+\frac{rH_2S}{\alpha_3}} + \frac{f_5 rH_2S}{1+rH_2S}. \quad (A.16)$$

This equation is solved algebraically for $r_{SO_4(in)}$ yielding Eq. (12) in the text, reproduced here as Eq. (A.17):

$$rSO_{4(in)} = \frac{rH_2S + rH_2S - f_5 rH_2S + \alpha_3 f_5 rH_2S}{\alpha_4[\alpha_3 + \alpha_3 rH_2S + f_5 rH_2S - \alpha_3 f_5 rH_2S]}. \quad (A.17)$$

Following the logic above, we can write a mass balance equation for the branch point differentiating the inside and outside of the cell (note this is identical to Eq. (A.5); see text for details):

$$\varphi_1 \frac{r_1}{1+r_1} = \varphi_2 \frac{r_2}{1+r_2} + \varphi_3 \frac{r_3}{1+r_3}. \quad (A.18)$$

As in the hypothetical case explored above, $\varphi_1 = \varphi_2 + \varphi_3$ and we define:

$$f_3 = \frac{\varphi_3}{\varphi_2 + \varphi_3} = \frac{\varphi_3}{\varphi_1}. \quad (A.19)$$

From Eqs. (A.10) and (A.19), we can rewrite Eq. (A.18) as:

$$\frac{rSO_{4(out)}\alpha_1}{1+rSO_{4(out)}\alpha_1} = (1-f_3)\frac{r_2}{1+r_2} + f_3 \frac{r_3}{1+r_3}. \quad (A.20)$$

The equalities, Eqs. (A.11) and (A.14), are substituted into Eq. (A.20), from which the isotope ratio of the external sulfate pool, $rSO_{4(out)}$, can be solved (also shown as Eq. (14) in the text):

$$rSO_{4(out)} = \frac{rSO_{4(in)} + rSO_{4(in)}rH_2S - f_3 rSO_{4(in)} + f_3 rH_2S}{\alpha_1[1 + rH_2S + f_3 rSO_{4(in)} - f_3 rH_2S]}. \quad (A.21)$$

References

Akagi, J.M., 1995. Respiratory sulfate reduction. In: Barton, L.L. (Ed.), *Sulfate-Reducing Bacteria*. Plenum Press, New York, pp. 89–109.

Brüchert, V., Knoblauch, C., Jørgensen, B.B., 2001. Controls on stable sulfur fractionation during bacterial sulfate reduction in Arctic sediments. *Geochim. Cosmochim. Acta* **65**, 763–776.

Brunner, B., Bernasconi, S.M., 2005. A revised isotope fractionation model for dissimilatory sulfate reduction in sulfate reducing bacteria. *Geochim. Cosmochim. Acta.* **69**, 4759–4771.

Canfield, D.E., 1989. Reactive iron in marine sediments. *Geochim. Cosmochim. Acta* **53**, 619–632.

Canfield, D.E., 2001a. Isotope fractionation by natural populations of sulfate-reducing bacteria. *Geochim. Cosmochim. Acta* **65**, 1117–1124.

Canfield, D.E., 2001b. Biogeochemistry of sulfur isotopes. In: Valley, J.W., Cole, D.R. (Eds.), *Reviews in Mineralogy and Geochemistry*, vol. 43. Mineralogical Society of America, Blacksburg, VA, pp. 607–636.

Canfield, D.E., Habicht, K.S., Thamdrup, B., 2000. The Archean sulfur cycle and the early history of atmospheric oxygen. *Science* **288**, 658–661.

Chambers, L.A., Trudinger, P.A., Smith, J.W., Burns, M.S., 1975. Fractionation of sulfur isotopes by continuous cultures of *Desulfovibrio desulfuricans*. *Canadian J. Microbiol.* **21**, 1602–1607.

Cline, J.D., 1969. Spectrophotometric determination of hydrogen sulfide in natural waters. *Limnol. Oceanogr.* **14**, 454–458.

Cox, R.P., Miller, M., Nielsen, J.B., Thomsen, J.K., 1989. Continuous turbidometric measurements of microbial cell-density in bioreactors using a light-emitting diode and a photodiode. *J. Microb. Methods* **10** (1), 25–31.

Cypionka, H., 1995. Solute transport and cell energetics. In: Barton, L.L. (Ed.), *Sulfate-Reducing Bacteria*. Plenum Press, New York, pp. 151–184.

Dahl, C., Trüper, H.G., 1994. Enzymes of dissimilatory sulfide oxidation in phototrophic sulfur bacteria. In: Peck, H.D., Jr.Jr., LeGall, J. (Eds.), *Methods in Enzymology. Inorganic Microbial Sulfur Metabolism*, vol. 243. Academic Press, San Diego, pp. 400–421.

Detmers, J., Brüchert, V., Habicht, K.S., Kuever, J., 2001. Diversity of sulfur isotope fractionations by sulfate-reducing prokaryotes. *Appl. Environ. Microbiol.* **67**, 888–894.

Ding, T., Valkiers, H., Kipphards, H., De Bièvre, P., Taylor, P.D.P., Gonfiantini, R., Krouse, R., 2001. Calibrated sulfur isotope abundance ratios of three IAEA sulfur isotope reference materials and V-CDT with a reassessment of the atomic weight of sulfur. *Geochim. Cosmochim. Acta* **65** (15), 2433–2437.

Farquhar, J., Johnston, D.T., Wing, B.A., Habicht, K.S., Canfield, D.E., Airieau, S., Thiemens, M.H., 2003. Multiple sulphur isotopic interpretations of biosynthetic pathways: implications for biological signatures in the sulphur isotope record. *Geobiology* **1**, 27–36.

Fossing, H., Jørgensen, B.B., 1989. Measurement of bacterial sulfate reduction in sediments: evaluation of a single-step chromium reduction method. *Biogeochemistry* **8**, 205–222.

Habicht, K.S., Canfield, D.E., 1997. Sulfur isotope fractionation during bacterial sulfate reduction in organic-rich sediments. *Geochim. Cosmochim. Acta* **61**, 5351–5361.

Habicht, K.S., Gade, M., Thamdrup, B., Berg, P., Canfield, D.E., 2002. Calibration of sulfate levels in the Archean ocean. *Science* **298**, 2372–2374.

Habicht, K.S., Salling, L., Thamdrup, B., Canfield, D.E., 2005. The effect of low sulfate concentrations and lactate oxidation on isotope fractionation during sulfate reduction by *Archaeoglobus fulgidus* strain Z. *Appl. Environ. Microbiol.* **71**, 3770–3777.

Harrison, A.G., Thode, H.G., 1958. Mechanisms of the bacterial reduction of sulfate from isotope fractiontion studies. *Trans. Faraday Soc.* **53**, 84–92.

Hayes, J.M., 2001. Fractionation of carbon and hydrogen isotopes in biosynthetic processes. In: Valley, J.W., Cole, D.R. (Eds.), *Rev. Mineral. Geochem.*, vol. 43. Mineralogical Society of America, Blacksburg, VA, pp. 225–277.

Hochachka, P.W., Somero, G.N., 1984. Temperature Adaptation. In: *Biochemical Adaptation*. Princeton University Press, Princeton, New Jersey, Kopi, pp. 355–449.

Ingraham, J.L., Marr, A.G., 1996. Effect of temperature, pressure, pH, and osmotic stress on growth. In: Neidhardt, F.C., Curtis, J.L., Lin, E.C.C., Brooks Low, K., Magasanik, B., Reznikoff, W.S., Riley, M., Schaechter, M., Umbarger, H.E. (Eds.), *Escherichia coli* and *Salmonella*, Cellular and Molecular Biology, vol. 2. ASM Press, Washington, DC, pp. 1578–1670.

Isaksen, M.F., Jørgensen, B.B., 1996. Adaptation of psychrophilic and psychrotrophic sulfate-reducing bacteria to permanently cold marine environments. *Appl. Environ. Microbiol.* **62** (2), 408–414.

Kaplan, I.R., Rittenberg, S.C., 1964. Microbiological fractionation of sulphur isotopes. *J. Gen. Microbiol.* **34**, 195–212.

Kemp, A.L.W., Thode, H.G., 1968. The mechanism of the bacterial reduction of sulphate and of sulphite from isotope fractionation studies. *Geochim. Cosmochim. Acta* **32**, 71–91.

Knoblauch, C., Jørgensen, B.B., 1999. Effect of temperature on sulphate reduction, growth rate and growth yield in five psychrophilic sulphate-reducing bacteria from Arctic sediments. *Environ. Microbiol.* **1** (5), 457–467.

Ohmoto, H., Felder, R.P., 1987. Bacterial activity in the warmer, sulphate-bearing, Archaean oceans. *Nature* **328**, 244–246.

Rabus, R., Hansen, T., Widdel, F., 2000. Dissimilatory sulfate- and sulfur-reducing prokaryotes. In: Balows, A., Trüper, H.G., Dworkin, M., Harder, W., Schleifer, K.-H. (Eds.), *The Prokaryotes: An Evolving Electronic Resource for the Microbiological Community*. third ed., release 3.3, September 8, 2000, Springer-Verlag, New York. Available from: <http://link.springer-ny.com/link/service/books/10125/>.

Rabus, R., Brüchert, V., Amann, J., Könneke, M., 2002. Physiological response to temperature changes of the marine, sulfate-reducing bacterium *Desulfobacterium autotrophicum*. *FEMS Microbiol. Ecol.* **42**, 409–417.

Rees, C.E., 1973. A steady-state model for sulphur isotope fractionation in bacterial reduction processes. *Geochim. Cosmochim. Acta* **37**, 1141–1162.

Scherer, S., Neuhaus, K., 2002. Life at low temperatures. In: Balows, A., Trüper, H.G., Dworkin, M., Harder, W., Schleifer, K.H. (Eds.), *The Prokaryotes: An Evolving Electronic Resource for the Microbiological Community*, third edition, release 3.9, April 1 2002, Springer, New York. Available from: <http://link.springer-ny.com/link/service/books/10125>.

Thode, H.G., Kleerekoper, H., McElcheran, D.E., 1951. Sulphur isotope fractionation in the bacterial reduction of sulphate. *Res. London* **4**, 581–582.

Widdel, F., 1988. Microbiology and ecology of sulfate-and sulfur-reducing bacteria. In: Zehnder, A.J.B. (Ed.), *Biology of Anaerobic Organisms*. John Wiley, New York, pp. 469–585.